ELSEVIER

Contents lists available at ScienceDirect

### Biosensors and Bioelectronics

journal homepage: http://www.elsevier.com/locate/bios





# Wireless, continuous monitoring of daily stress and management practice via soft bioelectronics

Hojoong Kim <sup>a, b</sup>, Yun-Soung Kim <sup>a</sup>, Musa Mahmood <sup>a</sup>, Shinjae Kwon <sup>a</sup>, Fayron Epps <sup>c</sup>, You Seung Rim <sup>b,\*\*</sup>, Woon-Hong Yeo <sup>a,d,e,\*</sup>

- a George W. Woodruff School of Mechanical Engineering, Institute for Electronics and Nanotechnology, Georgia Institute of Technology, Atlanta, GA, 30332, USA
- <sup>b</sup> Department of Intelligent Mechatronics Engineering, Sejong University, Seoul, 05006, Republic of Korea
- <sup>c</sup> Nell Hodgson Woodruff School of Nursing, Emory University, Atlanta, GA, 30322, USA
- d Wallace H. Coulter Department of Biomedical Engineering, Parker H. Petit Institute for Bioengineering and Biosciences, Georgia Institute of Technology, Atlanta, GA, 30332. USA
- <sup>e</sup> Center for Human-Centric Interfaces and Engineering, Neural Engineering Center, Institute for Materials, Institute for Robotics and Intelligent Machines, Georgia Institute of Technology, Atlanta, GA, 30332, USA

### ARTICLE INFO

# Keywords: Wireless soft electronics Continuous stress monitoring Stress management practice Galvanic skin response (GSR) Skin temperature

#### ABSTRACT

Stress has become a significant factor, directly affecting human health. Due to the numerous sources of stress that are inevitable in daily life, effective management of stress is essential to maintain a healthy life. Recent advancements in wearable devices allow monitoring stress levels via the detection of galvanic skin response on the skin. Some of these devices show the capability of assessing stress relief methods. However, prior works have been limited in a controlled laboratory setting with a short period assessment (<1 h) of stress intervention. The existing systems' main issues include motion artifacts and discomfort caused by rigid and bulky electronics and mandatory device connection on active fingers. Here, we introduce soft, wireless, skin-like electronics (SKINTRONICS) that offers continuous, portable daily stress and management practice monitoring. The ultrathin, lightweight, all-in-one device captures the change of a subject's stress over six continuous during everyday activities, including desk work, cleaning, and resting. At the same time, the SKINTRONICS proves that typical stress alleviation methods (mindfulness and meditation) can reduce stress levels, even in the middle of the day, which is supported by statistical analysis. The low-profile, wireless, gel-free device shows enhanced breathability and minimized motion artifacts compared to a commercial stress monitor. Collectively, this study shows the first demonstration of soft, nanomembrane bioelectronics for long-term, continuous assessment of stress and intervention effectiveness throughout daily life.

### 1. Introduction

Work-related stress and its adverse outcomes have resulted in severe risks to individuals and public health (Alberdi et al., 2016; Ebert et al., 2018). For example, excessive workplace stress caused 120,000 deaths, with \$190 billion in healthcare costs per year in the United States (Goh et al., 2016). Individuals with high levels of stress suffer from negative physical and psychological consequences, such as sleeping problems (Åkerstedt, 2006), depression (Heber et al., 2016; Kalia 2002), and cardiovascular disease (Can et al., 2019; McEwen 2008). Therefore,

early detection and management of excessive stress are critical to maintaining a healthy life. Stress levels have been estimated by a self-graded response or behavior data, which is subjective and hardly quantifiable (Can et al., 2019; Sharma and Gedeon 2012). Recently, to evaluate the effectiveness of stress management, wearable systems have been developed by measuring physiological signals from the heart, muscle, and brain (Can et al., 2019; Lim et al., 2020; Sharma and Gedeon 2012).

Electrodermal activity, also known as galvanic skin response (GSR), is one of the key indicators that directly evaluate stress arousal and

E-mail addresses: youseung@sejong.ac.kr (Y.S. Rim), whyeo@gatech.edu (W.-H. Yeo).

<sup>\*</sup> Corresponding author. Georgia Institute of Technology, Woodruff School of Mechanical Engineering, Center for Human-Centric Interfaces and Engineering, Atlanta, GA, 30332, USA

<sup>\*\*</sup> Corresponding author. Department of Intelligent Mechatronics Engineering, Sejong University, Seoul 05006, Republic of Korea

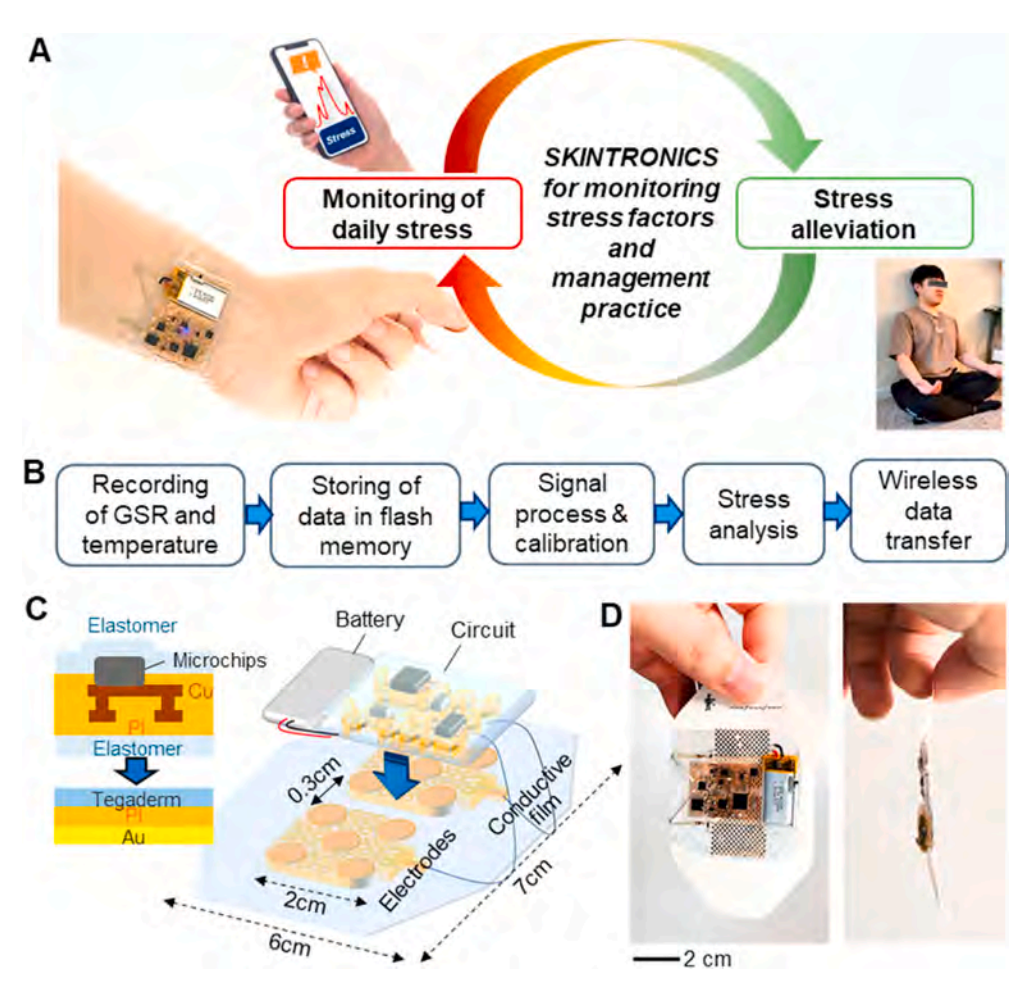


Fig. 1. Overview of wireless, continuous monitoring of daily stress and management practice via soft nanomembrane bioelectronics. A) SKINTRONICS for realtime, continuous monitoring of daily stress factors and management practice. B) Flowchart showing the use of SKINTRONICS for monitoring of GSR and temperature on the skin. C) Schematic illustration of the fully integrated device composed of a multilayered circuit, a pair of nanomembrane electrodes, and a rechargeable battery. D) Photos showing an ultrathin and flexible device in an angled view (left) and side view (right).

cognitive states by sensing the sympathetic nervous system (Cabibihan and Chauhan, 2017; Dehzangi et al., 2018; Hernando-Gallego et al., 2018). The cognitive and emotional stressor activates the sympathetic nervous system (SNS), promoting the eccrine glands' secretion to generate sweat on the skin (Boucsein, 2012). The GSR sensors can monitor the sympathetic activity by detecting the variation of the ionic permeability of sweat gland membranes (Fig. S1). The phasic signal of GSR, rapid time-varying response, is correlated with the arousals by SNS (Dehzangi et al., 2018; Hernando-Gallego et al., 2018). Thus, identification of the phasic component of GSR allows the quantification of the stress. GSR is typically measured by attaching wired gel-electrodes on fingers or hands where the sweat glands exist densely (Kappeler-Setz et al., 2011; Subramanian et al., 2018; Yin et al., 2019). However, these locations cause significant issues of motion artifacts and data loss from frequently disconnected wires. Recent advances in miniaturized wearable devices allow GSR's wireless detection on other areas, such as wrists and arms (Gautam et al., 2018; Olbrich et al., 2019). These devices, however, still suffer from side effects, including substantial motion artifacts caused by rigid sensor dissociation from the skin, skin irritation from electrolyte gels, and discomfort due to aggressive fixtures and straps (Herbert et al., 2018; Kwon et al., 2020; Lim et al., 2020). Recent reports show that wearable devices can measure stress intervention and the effectiveness of the management practice (Svetlov et al., 2019) (Yin et al., 2019) (Liu et al., 2019) (Fallon et al., 2020). Nevertheless, these devices still rely on bulky, rigid sensors and electronics, limiting the continuous and long-term use in daily life. In addition, all of those studies have been conducted in controlled laboratory environments with limited monitoring time, less than an hour.

This paper introduces a new class of technologies that develop soft, nanomembrane biosensors, and stretchable bioelectronics. The all-in-

one wearable device, named SKINTRONICS, offers wireless, portable, continuous, and long-term (>6 h) recording of GSR and temperature to assess stress on the skin during daily life. Also, the ultrathin and lightweight system can monitor stress management practice and the intervention efficacy via statistical analysis. The soft wearable device that makes conformal, intimate contact to the skin without electrolyte gels allows the recording of high-quality physiological data with minimized motion artifacts. A set of experimental studies proves the low-profile device's enhanced breathability along with no side effects to the skin after a 6-h long device wearing. Real-time monitoring of stress alleviation methods demonstrates the effectiveness of mindfulness of meditation to relieve stress in the middle of daily activities.

### 2. Materials and Methods

### 2.1. Fabrication of SKINTRONICS

Nanomembrane electrodes and stretchable circuits were fabricated using the combination of standard microfabrication, material transfer printing, and soft material packaging (Kim et al., 2019; Mahmood et al., 2019; Mishra et al., 2020). For the electrodes, Cr and Au were sputtered on a Si wafer and patterned into an open-mesh, meander structure, followed by etching steps. For the stretchable circuit fabrication, polyimide and polydimethylsiloxane (PI/PDMS) layers were spin-coated on a Si wafer. Then, the 1st Cu layer was deposited by sputtering and patterned into a serpentine mesh network. Additional layers (PI/Cu/PI) were deposited, and the 1st and the 2nd Cu layers were connected. Then, the circuit surface was etched by reactive ion etcher, leaving PI-insulated Cu traces and exposed Cu pads for subsequent soldering of electronic chip components. Additional details of the electrodes and

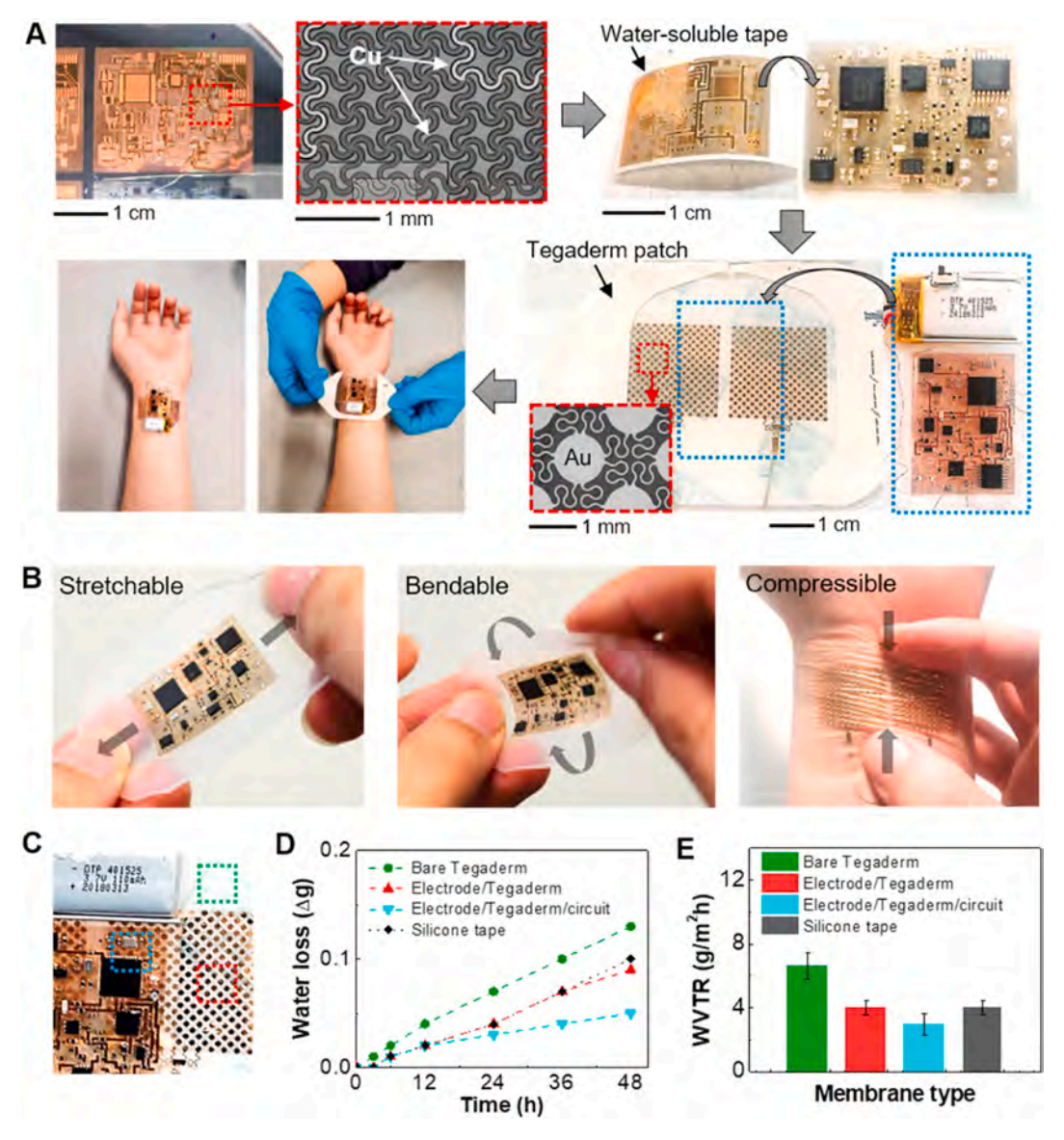


**Fig. 2. Fabrication, mechanical flexibility, and breathability of SKINTRONICS.** A) A multi-step fabrication process of SKINTRONICS: (step 1) preparation of circuit interconnects on a Si wafer via microfabrication, (step 2) transfer-printing of the interconnects on a soft elastomer, followed by integration of microchips, (step 3) integration with electrodes (red square) on a Tegaderm patch, along with a rechargeable battery (blue square), and (step 4) mounting of the device on the wrist for stress monitoring and management. B) Photos showing the device's stretchable, bendable, and compressible characteristics. C) Photo of a device with three different locations: case 1 – green, Tegaderm film only, case 2 – red, electrode only, and case 3 – blue, electrode and circuit. D) Results of water weight loss according to the membrane type, compared with a medical-grade, breathable silicone tape. E) Measured water-vapor transmission rates (WVTR) for four membrane types in D. (For interpretation of the references to color in this figure legend, the reader is referred to the Web version of this article.)

circuits' fabrication methods are summarized in Supplementary Note S1, Fig. S2, and Table S1.

### 2.2. Data recording, signal processing, and analysis

For stress monitoring, a fabricated SKINTRONICS was mounted on a subject's non-dominant hand's inner wrist. The SKINTRONCS measures GSR as the Wheatstone bridge's potential variation. A digital potentiometer actively moves a baseline potential to the central position in the detection range (0–1 V) to increase signal sensitivity. The sampling rate was varied from 1 to 5 Hz, depending on the target recording time. Recorded GSR data was stored directly onto the microcontroller's flash memory. For validation of the device performance, a commercial physiological monitor (BioRadio, Great Lakes NeuroTechnologies) was utilized with three gel-covered snap electrodes. These sensors were mounted on the middle phalanx of the index finger, the middle finger,

and the hand's back for grounding. An armband strap secured these sensors on the skin, connected to the BioRadio. The sampling rate was 250 Hz and averaged to 10 Hz for further analysis. The phasic components of GSR signals were extracted from raw data using the band-pass filter (0.2–1 Hz). The root-mean-square (RMS) value of the phasic components was calculated as a threshold level to detect GSR peaks. The peaks above the threshold were defined as stress arousals and those numbers were counted every minute. Signal-to-noise ratio (SNR) was calculated based on the phasic GSR and noise signals, including motion artifacts identified by the high-pass filter (1 Hz). After RMS conversion of both signals, SNR values (unit: dB) are calculated by the following equation:

$$SNR = 10Log_{10} \left( \frac{RMS\_signal}{RMS\_noise} \right)$$
 (1)

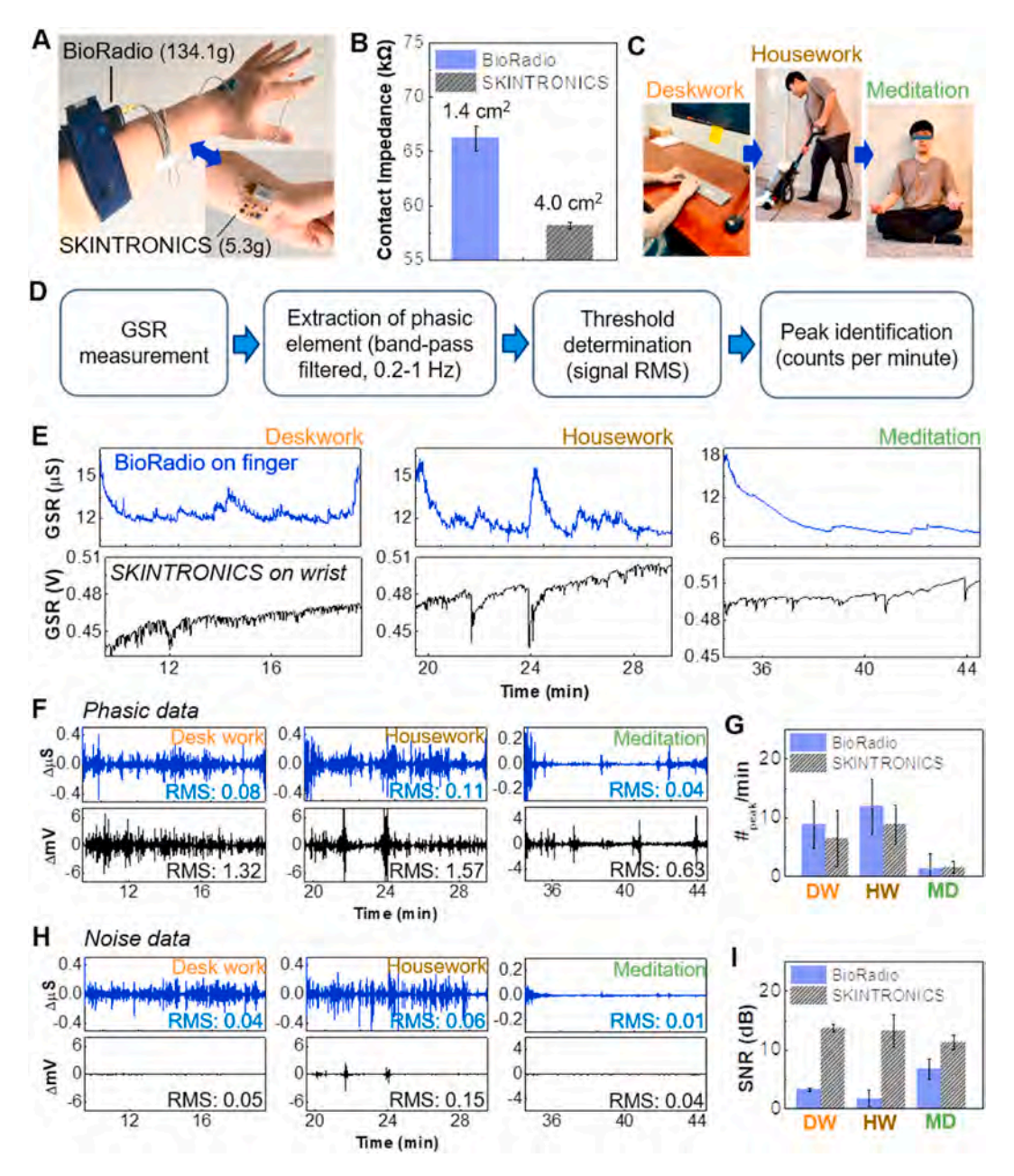


Fig. 3. Validation of the device performance compared to a commercial device on stress monitoring. A) Photo that compares the form factor and weight of two devices. B) Comparison of skin-electrode contact impedance. Error bars show standard deviation (n = 5). C) Three representative daily activities: deskwork (DW), housework (HW), and meditation (MD). D) Flowchart showing the data processing sequence. E) Raw GSR and F) their phasic signals measured by BioRadio (top) and SKINTRONICS (bottom). G) Number of peaks for three activities (n = 3). H) Noise data caused by motion artifacts. I) Comparison SNR values for three activities (n = 3).

### 2.3. Procedures for monitoring of stress in daily life

The all-in-one, low-profile SKINTRONICS offers portable, continuous monitoring of stress. Subjects were asked to wear the device on the inner wrist with multiple activities, such as deskwork (reading articles and data analysis) and vacuum cleaning. In addition, each subject attempted stress alleviation activities, such as mindfulness or meditation. For mindfulness, each subject was asked to maintain any restful activity for 10 min. For meditation, each subject was asked to turn on calm music, close the eyes, and keep their mind peaceful while concentrating on breathing for 10 min. We used a small lithium polymer battery (110 mAh) for the continuous data recording, integrated with the wearable device (Fig. S3). This battery could record both GSR and temperature up to 7 h. Afterward, a magnet-assisted connection was required to

recharge the battery. Overall, the human pilot study involved two healthy volunteers; the study followed the approved IRB (#H20204). All participants agreed and signed to the consent form to allow the experiment procedure.

### 3. Results and discussion

### 3.1. System architecture of SKINTRONICS and applications for daily stress management

In this study, we develop a wearable, wireless, all-in-one system (SKINTRONICS), which enables continuous, long-term monitoring of daily stress as well as a management practice for multiple days. Fig. 1A captures the overview of the use of SKINTRONICS on the skin for

monitoring stress factors and the effectiveness of stress alleviation practice throughout daily activities. The SKINTRONICS is composed of a pair of nanomembrane electrodes and a stretchable circuit enclosed by a soft elastomeric membrane. Overall, the device is ultrathin (<5 mm in thickness), lightweight (<6 g even with a battery), and low modulus (<100 kPa), providing an exceptionally small form factor for comfortable and long-term wearability on the skin. A flow chart in Fig. 1B illustrates the overall procedure to quantify stress levels based on GSR and temperature recording on the skin. The measured signals are stored in the flash memory of the on-board microcontroller chip. Temperature signals, measured on the skin, are used to compensate for undesirable GSR fluctuations due to the temperature change. Details of the device structure appear in Fig. 1C, which shows a multi-layered arrangement, including electrodes, conductive films, wireless circuit, rechargeable battery, soft encapsulant, and medical film. Flexible film cables connect the nanomembrane electrodes to the stretchable circuit on top of the soft elastomer. Photos in Fig. 1D captures the form factor of the fabricated SKINTRONICS, integrated with a clinical-grade medical tape for skin mounting.

### 3.2. Manufacturing, mechanical reliability, and breathability of SKINTRONICS

A series of optical microscope images and photos in Fig. 2A summarizes the device fabrication steps, including circuit preparation, transfer printing, electrodes integration, and skin mounting process. The fabrication of a microstructured circuit on a Si wafer follows the standard micromachining techniques with photolithography, metallization, and etching. We used an open-mesh, meander design to construct the circuit interconnects for mechanical flexibility and stretchability when mounted on the skin. A water-soluble tape facilitates the retrieval of the fabricated circuit patterns for transfer printing onto an elastomeric membrane. A follow-up integration of functional chips (microcontroller, analog front end, thermistor, digital potentiometer, and charging controller) finishes the circuit fabrication. The next step is to assemble the stretchable Au electrodes and circuits with a clinical-grade medical film (Tegaderm, 3 M,  $7 \times 6$  cm<sup>2</sup>). The electrodes are attached to the film's adhesive side while the circuit is placed on top of the film, facilitated by a gel elastomer (1:2 mixture of Ecoflex 00-30 and Gels, Smooth-On). A pair of GSR electrodes have 200 nm in thickness, with the pattern size  $2 \times 2 \text{ cm}^2$  and inter-distance of 0.3 cm between the pair. The circuit size is  $3.1 \times 2.2 \text{ cm}^2$ , with 2 mm in thickness. The total thickness of the SKINTRONICS, including a rechargeable battery, is less than 5 mm. For continuous monitoring of stress, we mounted the SKINTRONICS on the inner wrist. Details of the circuit design and electronic wiring appear in Figs. S4 and S5, respectively.

Collective photos in Fig. 2B capture the mechanical characteristics of the compliant circuit and electrodes, which can endure stretching, bending, and compression without mechanical failure. The open-mesh structures, used in both electrodes and circuits, accommodate applied strains from bending and stretching. Considering the continuous use of the wearable device, it is critical to validate the mechanical robustness. Our prior work proves the electrode's functionality with 30% uniaxial stretching up to 400 cycles (Kim et al., 2019). Also, a mechanical stretching test in Fig. S6 shows the circuit's maximum stretchability over 20% and reliability upon repeated tensile strain (10%) over 500 cycles. The measured electrical signals show negligible changes.

Another essential feature of a wearable device is the breathability for long-term wearing on the skin (Mishra et al., 2017; Sun et al., 2018). The ability to allow air permeation through the membrane improves prolonged adhesion of the device as well as minimized skin irritation. The experimental results in Fig. 2C–E shows the characterized breathability of materials via measured changes of water loss. There are four membrane types, including Tegaderm film only, electrodes with the film, electrodes and circuit with the film, and another clinical-grade silicone film (Kind Removal, 3 M). In this study, we measured the change of

water vapor transmission rate (WVTR) over time, details of the experimental method in Fig. S7. WVTR for each membrane was measured at the constant temperature (24 °C) and humidity (50%). The graph in Fig. 2D shows water loss per each case over 48 h. WVTR is calculated by the following equation (Hu et al., 2019):

$$WVTR = \frac{\Delta g}{A \times t} \tag{2}$$

where  $\Delta g$ , A, and t are the weight changes of water, membrane area, and elapsed time, respectively. As summarized in Fig. 2E, the laminated circuit and electrode slightly decrease the values. However, the fully integrated membrane with additional components still shows a similar WVTR level as the clinical-grade, breathable silicone tape, demonstrating the device feasibility for multi-hour use on the skin. Collectively, the presented experimental results in Fig. 2 show the acceptable ranges of mechanical reliability and breathability of the SKINTRONICS for a pilot study with human subjects.

### 3.3. Validation of the device performance on stress monitoring

In this study, we validate the performance of SKINTRONICS on stress monitoring with human subjects. Specifically, Fig. 3 summarizes the side-to-side comparison of recorded data between SKINTRONICS and a clinical-grade commercial device (BioRadio, Great Lakes Neuro-Technologies). Fig. 3A captures the exceptionally small form factor of the SKINTRONICS on the inner wrist compared to the commercial wearable system that wirelessly transfers GSR signals via Bluetooth. The commercial system utilizes a pair of gel-covered rigid electrodes mounted on two fingers and a data acquisition module, worn on the arm. The wireless, all-in-one SKINTRONICS (5.3 g) is about 25 times lighter than the BioRadio (134.1 g) with multiple electronic components connected by wires. The skin-electrode contact impedance in Fig. 3B shows the difference between two devices where the lowered value from SKINTRONICS is caused by the highly conformal contact of large-area electrodes. In this study, we increased the electrode size of SKIN-TRONICS up to 4.0 cm<sup>2</sup> compared to the gel (1.4 cm<sup>2</sup>) to enhance the areal coverage. As a result, the dry, skin-like electrode shows a lower skin-electrode contact impedance than the gel electrode on the finger.

Fig. 3C captures three representative daily activities that a subject follows while measuring GSR signals from both devices simultaneously. Recorded data are analyzed by going through the multi-step processes, as described in Fig. 3D, including phasic element extraction, threshold determination, and peak identification. A set of graphs in Fig. 3E presents raw GSR data, measured by BioRadio on fingers and SKINTRONICS on the wrist from three activities: deskwork, housework, and meditation (details in Materials and Methods). Fig. 3F summarizes the collected data after the extraction of phasic elements with RMS values. The average numbers of peaks counted from different activities in Fig. 3G show a significant reduction in peak numbers during meditation (1.61 and 1.33 for SKINTRONICS and BioRadio, respectively), compared to during other work-related activities (6.53-8.90 and 8.83-11.90). The result validates that both deskwork and housework cause stress to the user, while the stationary meditation effectively reduces the stress values significantly. Note that the counted number of peaks from Bio-Radio is higher than that from SKINTRONICS because fingers have more sweat glands than the wrist (Payne et al., 2016). Three times of the GSR measurements by SKINTRONICS with replacing electrodes show reliable data recording.

Considering real-time, continuous monitoring of GSR in daily life, it is critical to minimize noise, mostly from motion artifacts (Kwon et al., 2020; Lim et al., 2020; Mahmood et al., 2019). The lightweight, soft, skin-conformal SKINTRONICS demonstrates minimal effects from motion artifacts compared to BioRadio, as summarized in Fig. 3H and I. The conductive gel on a rigid sensor has drift motions at the interface during daily activities, while wires and other electronic components are

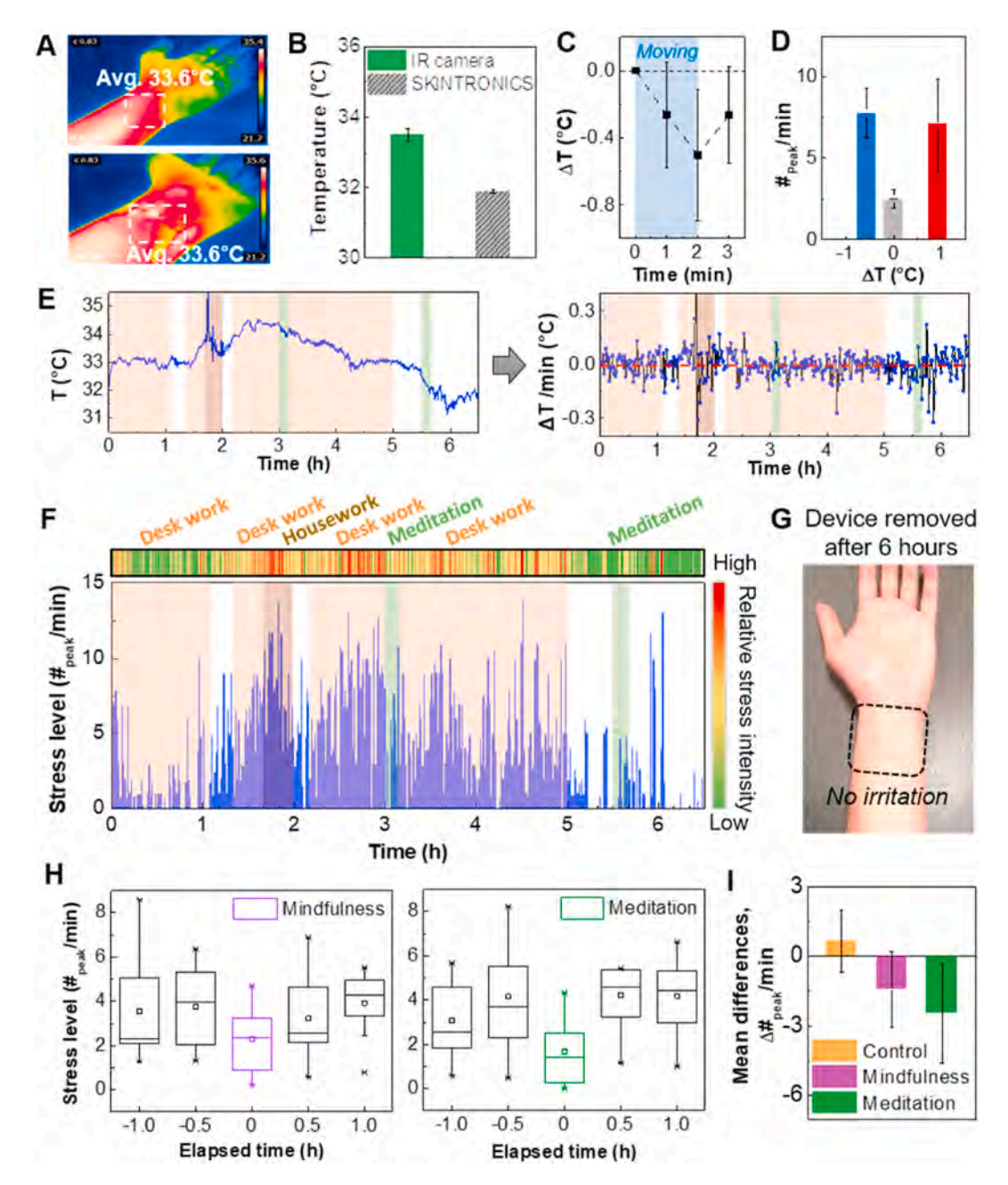


Fig. 4. Long-term recording of stress and effectiveness of management practice. A) Thermographic images of the inner wrist without (top) and with SKIN-TRONICS (bottom). The average temperature value is calculated from the indicated area in the white box. B) Comparison of measured temperature by an IR camera and SKINTRONICS. Error bars show standard deviation (n = 3). C) Temperature variation with moving activity (n = 3). D) Temperature effects on the number of stress peaks (n = 3). E) Continuously measured skin temperature by SKINTRONICS for over 6 h (left) and averaged variation per minute (right). F) Temperature-calibrated stress levels during multiple daily activities with deskwork, housework, and meditation. The upper bar displays a visualized stress intensity according to the measured stress peaks. G) Photo showing no side effects of the wearable device on the skin after 6 h. H) Comparison of two types of stress alleviation: mindfulness (left) and meditation (right), measured for 6 days with two subjects. Each stress level is averaged within 0.5 h prior and post to the alleviation. I) Calculated effectiveness of stress management practice. Control data shows no alleviation activity.

susceptible to movements during deskwork and housework. Overall, the set of experimental studies in Fig. 3 validates the enhanced performance of the SKINTRONICS in wireless, continuous, and ambulatory monitoring of GSR with negligible motion artifacts.

### 3.4. Long-term recording of stress and the effectiveness of management practice

The human body has the function of thermoregulation that actively controls body temperature by sweating through the skin. In other words,

GSR signals, measuring the change of skin conductance on sweat glands, are affected by the variation of body temperature (Doberenz et al., 2011; Gerrett et al., 2019). The uncontrollable ambient temperature must be carefully considered when measuring ambulatory GSR during a subject's daily life. As shown in Fig. 1, SKINTRONICS includes two sensors that measure GSR and skin temperature simultaneously to compensate for undesirable thermal effects during everyday activities.

Photos in Fig. 4A show thermographic images of the inner wrist without (top) and with (bottom) SKINTRONICS, captured by an infrared camera (E8, FLIR). Compared to the camera, the temperature sensor in

 Table 1

 Comparison of wearable stress detection sensors and intervention methods.

Reference	Device type (electrode)	Device location	Stress inducing method	Stress alleviating method	Intervention effectiveness (Amean)	Statistical values	Intervention monitoring time	Data recording place
This work	Soft, stretchable patch (dry electrode)	Wrist	Working (desk work/ housework)	Meditation/ mindfulness	60%/38%	F = 7.72, p = 0.003 (two-way ANOVA)	>6 h	Home/ Laboratory
Svetlov et al. (2019)	Rigid, wristband (dry electrode)	Wrist	Word memorization	Mindfulness relaxation	49%	Not applicable	40 min	Laboratory
Yin et al. (2019)	Rigid, wristband (gel electrode)	Palm	VR	VR	4%	Not applicable	52 min	Laboratory
Liu et al. (2019)	Rigid, bulky electronics (gel electrode)	Finger	TSST	Watching a video	43%	F = 5.27, p = 0.001 (multivariate ANOVA)	<60 min	Laboratory
Fallon et al. (2020)	Rigid, bulky electronics (gel electrode)	Finger	TSST	Music therapy	8–23%	F = 5.10, p < 0.01 (two-way ANOVA)	20 min	Laboratory
Akmandor and Jha (2017)	Rigid, bulky electronics (gel electrode)	Finger	Memory game, fly sound, ice test, and picture system	Music, warm stone, meditation, and news	49%	Not applicable	64 min	Laboratory

VR: virtual reality, TSST: trier social stress test, and ANOVA: analysis of variance.

SKINTRONICS shows lower values (Fig. 4B), caused by the device encapsulants that absorb and distribute external thermal energy. Moving activity results in temperature reduction (Fig. 4C), which is also confirmed by the thermal camera (Fig. S8). Temperature change, departed from normal lukewarm level, causes the GSR signal boost in the peak counting (Fig. 4D). These results indicate that constant moving and other daily life activities can overestimate the stress level, showing the importance of simultaneous temperature recording for necessary compensation. Fig. 4E shows temperature data (left) measured during daily activities over 6 h and averaged variation per minute (right). Fig. 4F summarizes a set of stress levels by counting GSR peaks per minute during multiple tasks, including desk work, housework, and meditation. Note that the number of GSR peaks include the compensation of temperature variation, while the colorized scale shows the level of stress intensity from high (red color) to low (green color). The stress level increases gradually with continuous deskwork. At the elapsed time between 1.5 and 3 h, the stress level becomes extremely high as the various work-related events are experienced. After meditation at 3 h, the stress level is decreased and lower than the initial work period. Another meditation after 5 h causes the lowest stress level for the subject. The SKINTRONICS, enclosed by a medical film (Tegaderm), is designed for a single-use since it loses the adhesion when detached from the skin. Considering possible reuse of the device, we developed another type of SKINTRONICS encapsulated by a reusable silicone tape (Kind Removal, 3 M), which offered multiple uses more than three times (Fig. S9). The reusable device measures continuous, high-quality GSR signals during multiple activities and meditation.

The breathable SKINTRONICS with good air permeability (studied in Fig. 2) shows no skin irritation and allergic reaction after the continuous use over 6 h (Fig. 4G). The novelty of real-time, continuous recording with SKINTRONICS is summarized in Fig. 4H and I, which can quantify the effectiveness of stress management practice such as mindfulness and meditation. Fig. 4H presents various stress levels from two subjects who use two types of stress alleviation methods for six days. Video S1 captures real-time, continuous monitoring of GSR and temperature during meditation and desk work. Details of the measured data appear in Figs. S10 and S11. Each work-related stress level is averaged within 0.5 h prior and post to the alleviation activities. Fig. 4I compares each alleviation method's efficacy via the mean difference of stress indicators, showing more effective stress reduction from meditation (60%) than mindfulness (38%). To confirm the impact of stress management, we used statistical analysis by using a two-way analysis of variance (Christensen 2020; Liu et al., 2019). The univariate assessment finds a significant effect on the alleviation activities as F = 7.72, p = 0.003 ( $\alpha =$ 0.05) where *F* value is the ratio of the variance of group means over the average values in group variances, p is the evidence for a hypothesis, and  $\alpha$  is the confidence level. Table 1 compares the performance of SKINTRONICS with other wearable stress monitors and intervention methods. High F ratio in this work clearly shows significant alleviation of stress with reliability (smaller p-value than  $\alpha$  value). This study collectively shows the first demonstration of a soft, wearable biosystem for long-term (>6 h), continuous assessment of stress, and intervention effectiveness throughout daily life.

### 4. Conclusion

This paper reports an all-in-one, wireless, soft bioelectronic system for portable, continuous monitoring of stress and management practice in daily life. The fully integrated stretchable system incorporates skin-conformal nanomembrane electrodes and wireless circuits. The wearable device on the wrist measures high-fidelity GSR and temperature with minimized motion artifacts and enhanced breathability, compared to a commercial device. Simultaneous skin temperature recording provides accurate detection of stress by removing unwanted contributions of temperature changes from sweating. In vivo demonstration with human subjects captures the device performance of continuous stress detection over 6 h during multiple daily activities, including desk work, cleaning, and stress alleviation. Collectively, the bioelectronic stress monitor, presented in this work, would provide a novel wearable platform for users to monitor daily stress factors actively and control them via management practice.

### CRediT authorship contribution statement

Hojoong Kim: Conceptualization, Formal analysis, Writing - original draft, conceived and designed the research, performed the experiments, analyzed the data, wrote the paper. Yun-Soung Kim: Writing - original draft, performed the experiments. Musa Mahmood: performed the experiments. Shinjae Kwon: performed the experiments. Fayron Epps: Formal analysis, Writing - original draft, analyzed the data. You Seung Rim: Writing - original draft, wrote the paper. Woon-Hong Yeo: Conceptualization, Writing - original draft, conceived and designed the research, wrote the paper.

### Declaration of competing interest

The authors declare the following financial interests/personal relationships which may be considered as potential competing interests: Georgia Tech has a pending US patent application.

#### Acknowledgments

W.-H.Y. acknowledges the support by the Goizueta Alzheimer's Disease Research Center (P50 AG025688). This work was partially supported by the National Science Foundation (grant NRI-2024742) and the Georgia Tech IEN Center Grant. This work was performed in part at the Institute for Electronics and Nanotechnology, a member of the National Nanotechnology Coordinated Infrastructure, which is supported by the National Science Foundation (Grant ECCS-2025462). H.K. acknowledges the support by the Basic Science Research Program through the National Research Foundation of Korea (NRF) funded by the Ministry of Education (NRF-2019R1A6A3A01096242).

### Appendix A. Supplementary data

Supplementary data to this article can be found online at https://doi.org/10.1016/j.bios.2020.112764.

#### References

- Åkerstedt, T., 2006. Psychosocial stress and impaired sleep. Scand. J. Work. Environ. Hea. 32 (6), 493–501.
- Akmandor, A.O., Jha, N.K., 2017. Keep the stress away with SoDA: stress detection and alleviation system. IEEE Trans. Multi-Scale Comput. Syst. 3 (4), 269–282.
- Alberdi, A., Aztiria, A., Basarab, A., 2016. Towards an automatic early stress recognition system for office environments based on multimodal measurements: a review. J. Biomed. Inf. 59, 49–75.
- Boucsein, W., 2012. Electrodermal Activity. Springer Science & Business Media.
   Cabibihan, J.-J., Chauhan, S.S., 2017. Physiological responses to affective tele-touch during induced emotional stimuli. IEEE T. Affect. Comput. 8 (1), 108–118.
- Can, Y.S., Arnrich, B., Ersoy, C., 2019. Stress detection in daily life scenarios using smart phones and wearable sensors: a survey. J. Biomed. Inf. 92, 103139.
- Christensen, R., 2020. One-way ANOVA. Plane Answers to Complex Questions. Springer, pp. 107–121.
- Dehzangi, O., Rajendra, V., Taherisadr, M., 2018. Wearable driver distraction identification on-the-road via continuous decomposition of galvanic skin responses. Sensors 18 (2).
- Doberenz, S., Roth, W.T., Wollburg, E., Maslowski, N.I., Kim, S., 2011. Methodological considerations in ambulatory skin conductance monitoring. Int. J. Psychophysiol. 80 (2) 87–95
- Ebert, D.D., Kahlke, F., Buntrock, C., Berking, M., Smit, F., Heber, E., Baumeister, H., Funk, B., Riper, H., Lehr, D., 2018. A health economic outcome evaluation of an internet-based mobile-supported stress management intervention for employees. Scand. J. Work. Environ. Health. 44 (2), 171–182.
- Fallon, V.T., Rubenstein, S., Warfield, R., Ennerfelt, H., Hearn, B., Leaver, E., 2020. Stress reduction from a musical intervention. Psycho. 30 (1), 20–27.
- Gautam, A., Simoes-Capela, N., Schiavone, G., Acharyya, A., de Raedt, W., Van Hoof, C., 2018. A data driven empirical iterative algorithm for GSR signal pre-processing. In: 26th European Signal Processing Conference (EUSIPCO), pp. 1162–1166.
- Gerrett, N., Amano, T., Havenith, G., Inoue, Y., Kondo, N., 2019. The influence of local skin temperature on the sweat glands maximum ion reabsorption rate. Eur. J. Appl. Physiol. 119 (3), 685–695.
- Goh, J., Pfeffer, J., Zenios, S.A., 2016. The relationship between workplace stressors and mortality and health costs in the United States. Manag. Sci. 62 (2), 608–628.
- Heber, E., Lehr, D., Ebert, D.D., Berking, M., Riper, H., 2016. Web-based and mobile stress management intervention for employees: a randomized controlled trial. J. Med. Internet Res. 18 (1), e21.

- Herbert, R., Kim, J.-H., Kim, Y.S., Lee, H.M., Yeo, W.-H., 2018. Soft material-enabled, flexible hybrid electronics for medicine, healthcare, and human-machine interfaces. Materials 11 (2), 187.
- Hernando-Gallego, F., Luengo, D., Artes-Rodriguez, A., 2018. Feature extraction of galvanic skin responses by nonnegative sparse deconvolution. IEEE J. Biomed. Hea. Inf. 22 (5), 1385–1394.
- Hu, X., Jia, X., Zhi, C., Jin, Z., Miao, M., 2019. Improving the properties of starch-based antimicrobial composite films using ZnO-chitosan nanoparticles. Carbohydr. Polym. 210, 204–209.
- Kalia, M., 2002. Assessing the economic impact of stress [mdash] the modern day hidden epidemic. Metabol. 51 (6), 49–53.
- Kappeler-Setz, C., Gravenhorst, F., Schumm, J., Arnrich, B., Tröster, G., 2011. Towards long term monitoring of electrodermal activity in daily life. Pers. Ubiquit. Comput. 17 (2), 261–271.
- Kim, Y.S., Mahmood, M., Lee, Y., Kim, N.K., Kwon, S., Herbert, R., Kim, D., Cho, H.C., Yeo, W.H., 2019. All-in-One, wireless, stretchable hybrid electronics for smart, connected, and ambulatory physiological monitoring. Adv. Sci. 6 (17), 1900939.
- Kwon, S., Kwon, Y.-T., Kim, Y.-S., Lim, H.-R., Mahmood, M., Yeo, W.-H., 2020. Skin-conformal, soft material-enabled bioelectronic system with minimized motion artifacts for reliable health and performance monitoring of athletes. Biosens. Bioelectron. 151, 111981.
- Lim, H.R., Kim, H.S., Qazi, R., Kwon, Y.T., Jeong, J.W., Yeo, W.H., 2020. Advanced soft materials, sensor integrations, and applications of wearable flexible hybrid electronics in healthcare, energy, and environment. Adv. Mater. 32 (15), e1901924.
- Liu, J.J.W., Reed, M., Vickers, K., 2019. Reframing the individual stress response: balancing our knowledge of stress to improve responsivity to stressors. Stress Health 35 (5), 607–616.
- Mahmood, M., Mzurikwao, D., Kim, Y.-S., Lee, Y., Mishra, S., Herbert, R., Duarte, A., Ang, C.S., Yeo, W.-H., 2019. Fully portable and wireless universal brain–machine interfaces enabled by flexible scalp electronics and deep learning algorithm. Nat. Mac. Intel. 1 (9), 412–422.
- McEwen, B.S., 2008. Central effects of stress hormones in health and disease: understanding the protective and damaging effects of stress and stress mediators. Eur. J. Pharmacol. 583 (2–3), 174–185.
- Mishra, S., Kim, Y.-S., Intarasirisawat, J., Kwon, Y.-T., Lee, Y., Mahmood, M., Lim, H.-R., Herbert, R., Yu, K.J., Ang, C.S., 2020. Soft, wireless periocular wearable electronics for real-time detection of eye vergence in a virtual reality toward mobile eye therapies. Sci. Adv. 6 (11) eaay1729.
- Mishra, S., Norton, J.J.S., Lee, Y., Lee, D.S., Agee, N., Chen, Y., Chun, Y., Yeo, W.H., 2017. Soft, conformal bioelectronics for a wireless human-wheelchair interface. Biosens. Bioelectron. 91, 796–803.
- Olbrich, S., Jahn, I., Stengler, K., 2019. Exposure and response prevention therapy augmented with naltrexone in kleptomania: a controlled case study using galvanic skin response for monitoring. Behav. Cognit. Psychother. 47 (5), 622–627.
- Payne, A.F., Schell, A.M., Dawson, M.E., 2016. Lapses in skin conductance responding across anatomical sites: comparison of fingers, feet, forehead, and wrist. Psychophysiology 53 (7), 1084–1092.
- Sharma, N., Gedeon, T., 2012. Objective measures, sensors and computational techniques for stress recognition and classification: a survey. Comput. Meth. Progr. Biomed. 108 (3), 1287–1301.
- Subramanian, R., Wache, J., Abadi, M.K., Vieriu, R.L., Winkler, S., Sebe, N., 2018. ASCERTAIN: emotion and personality recognition using commercial sensors. IEEE T. Affect. Comput. 9 (2), 147–160.
- Sun, B., McCay, R.N., Goswami, S., Xu, Y., Zhang, C., Ling, Y., Lin, J., Yan, Z., 2018. Gaspermeable, multifunctional on-skin electronics based on laser-induced porous graphene and sugar-templated elastomer sponges. Adv. Mater. 30 (50), 1804327.
- Svetlov, A.S., Nelson, M.M., Antonenko, P.D., McNamara, J.P.H., Bussing, R., 2019. Commercial mindfulness aid does not aid short-term stress reduction compared to unassisted relaxation. Heli. 5 (3), e01351.
- Yin, J., Arfaei, N., MacNaughton, P., Catalano, P.J., Allen, J.G., Spengler, J.D., 2019. Effects of biophilic interventions in office on stress reaction and cognitive function: a randomized crossover study in virtual reality. Indoor Air 29 (6), 1028–1039.

### **Supplementary Information**

## Wireless, Continuous Monitoring of Daily Stress and Management Practice via Soft Bioelectronics

Hojoong Kim<sup>a,b</sup>, Yun-Soung Kim<sup>a</sup>, Musa Mahmood<sup>a</sup>, Shinjae Kwon<sup>a</sup>, Fayron Epps<sup>c</sup>, You Seung Rim<sup>b,\*</sup>, and Woon-Hong Yeo<sup>a,d,e,\*</sup>

- <sup>a</sup> George W. Woodruff School of Mechanical Engineering, Institute for Electronics and Nanotechnology, Georgia Institute of Technology, Atlanta, GA 30332, USA
- <sup>b</sup> Department of Intelligent Mechatronics Engineering, Sejong University, Seoul 05006, Republic of Korea
- <sup>c</sup> Nell Hodgson Woodruff School of Nursing, Emory University, Atlanta, GA 30322, USA
- <sup>d</sup> Wallace H. Coulter Department of Biomedical Engineering and Parker H. Petit Institute for Bioengineering and Biosciences, Georgia Institute of Technology, Atlanta, GA 30332, USA
- <sup>e</sup> Center for Human-Centric Interfaces and Engineering, Neural Engineering Center, Institute for Materials, and Institute for Robotics and Intelligent Machines, Georgia Institute of Technology, Atlanta, GA 30332, USA
- \*Corresponding author: youseung@sejong.ac.kr (YSR) or whyeo@gatech.edu (W.-H.Y)

### Note S1. Fabrication of SKINTRONICS

### 1.1 Fabrication of circuits

- 1. Spin-coat PDMS (4:1 base-curing-agent ratio) on a Si wafer at 4000 RPM for 30 s.
- 2. Oxygen plasma treatment on PDMS surface for 8 s.
- 3. Spin-coat 1<sup>st</sup> polyimide layer (PI, PI-2610, HD MicroSystems) at 2000 RPM for 60 s (4.3 µm thickness).
- 4. Soft bake at 100 °C for 5 min and hard bake at 250°C for 1 h.
- 5. Deposit 0.5 µm thickness of Cu by sputtering.
- Spin-coat photoresist (PR, Microposit SC1813, MicroChem) at 3000 RPM for 30 s, and soft bake at 100°C for 5 min. Align with a photomask and expose UV light with intensity of 15 mJ/cm² for 12 s and develop with a developer (MF-319, MicroChem).
- 7. Etch Cu with Cu etchant (APS-100, Transene) and remove remaining PR with acetone, rinse with IPA and DI water.
- 8. Spin-coat 2<sup>nd</sup> PI layer (PI-2545, HD MicroSystems) at 2000 RPM for 60 s (3 μm thickness), and soft bake at 100°C for 5 min. Hard bake at 240 °C for 1 h in a vacuum oven.
- 9. Spin-coat PR (AZ P4620, Integrated Micro Materials) at 2000 RPM for 30 sec, and soft bake at 90°C for 4 min. Photolithography exposing UV light with intensity of 15 mJ/cm² for 100 s. Develop with a developer (AZ-400K, Integrated Micro Materials) diluted with DI water (AZ-400K:DI water = 1:4).
- 10. Etch for via hole with reactive ion etcher (RIE) at 250 W, 150 mTorr, and 20 sccm of oxygen for 15 min. Rinse with acetone, IPA, and DI water.
- 11. Deposit 1.7 µm thickness of 2<sup>nd</sup> Cu by sputtering.
- 12. Spin-coat PR (AZ P4620) at 1500 RPM for 30 s, and soft bake at 90°C for 4 min. Photolithography exposing UV light with intensity of 15 mJ/cm² for 120 s and develop.
- 13. Etch exposed Cu with Cu etchant. Remove PR with acetone, and rinse with IPA and DI water.
- 14. Spin-coat 3<sup>rd</sup> PI layer (PI-2610) at 3000 RPM for 60 s (2.7 μm thickness). Soft bake at 100°C for 5 min and hard bake at 240°C for 1 h in a vacuum oven.

- 15. Spin-coat PR (AZ P4620) at 900 RPM for 30 sec, and soft bakes at 90°C for 4 min. Photolithography exposing UV light with intensity of 15 mJ/cm² for 160 s and develop.
- 16. Etch exposed PI with RIE at 250 W, 150 mTorr, and 20 sccm of oxygen for 30 min. Remove remaining PR with acetone, and rinse with IPA and DI water.
- 17. Peel off the microfabricated circuit with a water-soluble tape (ASWT-2, Aquasol) from the PDMS/Si wafer and put on the 1 mm thickness of silicone elastomer (1:2 mixture of Ecoflex 00-30 and Gels, Smooth-On). Washing the tape with DI water.
- 18. Mount microchip components with screen-print low-temperature solder paste (alloy of Sn/Bi/Ag (42%/57.6%/0.4%), ChipQuik Inc.). Bake solder at 170 °C for 2 min.
- 19. Download firmware and flash a device through program line connected to circuit with magnetic cubes.

### 1.2 Fabrication of electrodes

- 1. Spin-coat PDMS (4:1 base-curing-agent ratio) on a Si wafer at 4000 RPM for 30 s.
- 2. Oxygen plasma treatment on PDMS surface for 8 s.
- 3. Spin-coat  $1^{st}$  polyimide layer (PI-2610) at 2000 RPM for 60 s (4.3  $\mu$ m thickness).
- 4. Soft bake at 100 °C for 5 min and hard bake at 250 °C for 1 h.
- 5. Deposited Cr/Au by sputtering (5/200 nm thickness).
- 6. Spin-coat PR (SC1813) at 3000 RPM for 30 s, and soft bake at 100°C for 3 min. Photolithography exposing UV light with intensity of 15 mJ/cm² for 12 s and develop with a developer (MF-319).
- 7. Etch Cr/Au by etchant (Chrome Mask Etchant 9030 and GE-8110, Transene) and remove remaining PR with acetone, rinse with IPA and DI water.
- 8. Spin-coat 2<sup>nd</sup> PI layer (PI-2545) at 2000 RPM for 60 s (3 μm thickness), and soft bake at 100°C for 5 min. Hard bake at 240 °C for 3 h in a vacuum oven.
- Spin-coat PR (AZ P4620) at 2000 RPM for 30 sec, and soft bakes at 90°C for 4 min. Photolithography with exposing UV light with intensity of 15 mJ/cm² for 100 s. Develop with a developer

- 10. Etch exposed PI except protection layer with RIE at 250 W, 150 mTorr, and 20 sccm of oxygen for 15 min. Remove remaining PR with acetone and rinse with IPA and DI water.
- 11. Peel off the microfabricated electrodes from the PDMS/Si wafer with a water-soluble tape and put on a medical patch (Tegaderm, 3M, <1 mm thickness). Wash the tape with DI water.
- 12. Connecting the electrodes to the Cu pads of the circuit through a flexible conductive film (ACF, 3M) attached by a silver paste.

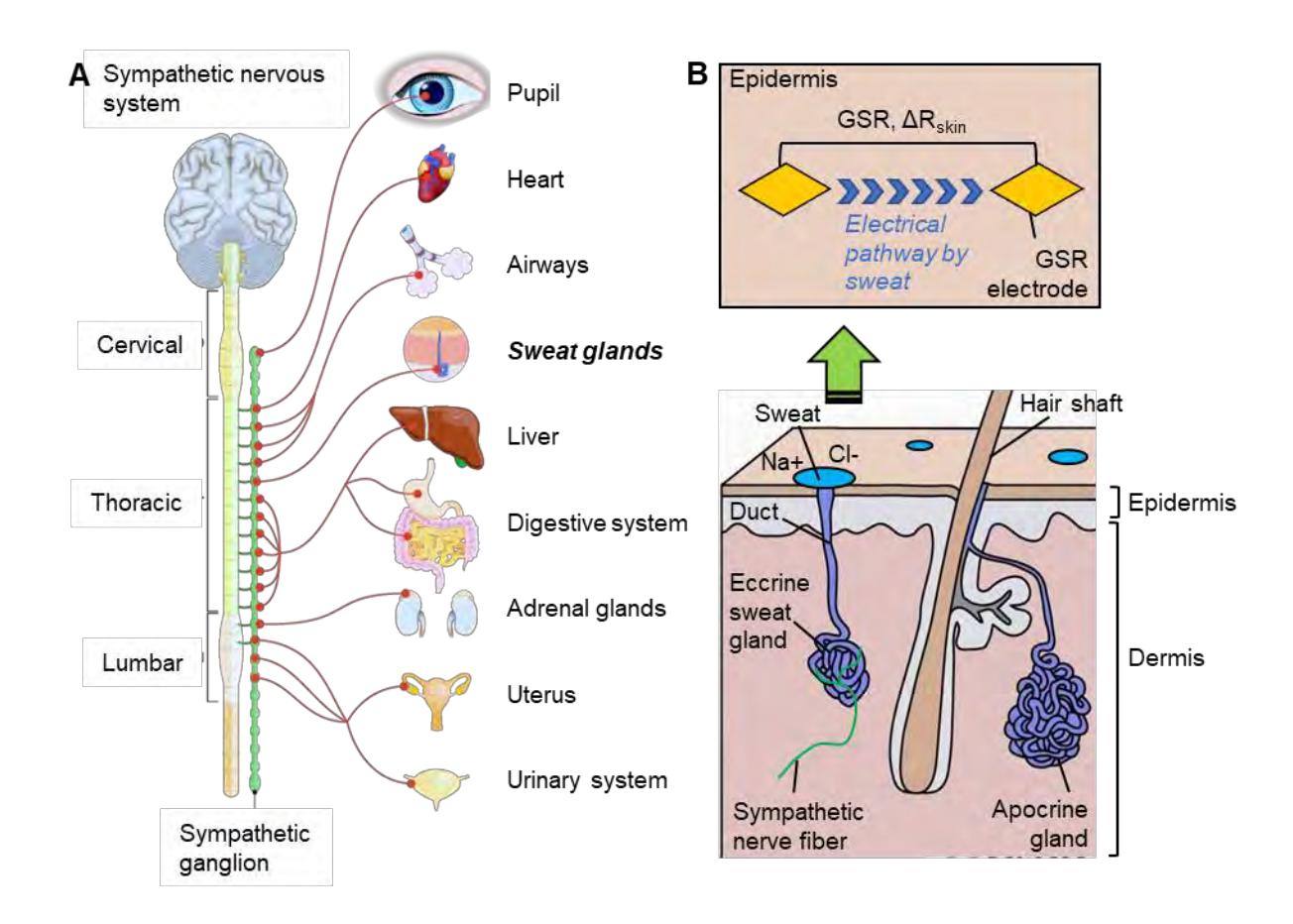


**Fig. S1.** The principle of GSR measurement. A) Sympathetic nervous system and its effect on various body organs. B) The secretion of eccrine sweat glands for GSR measurement.

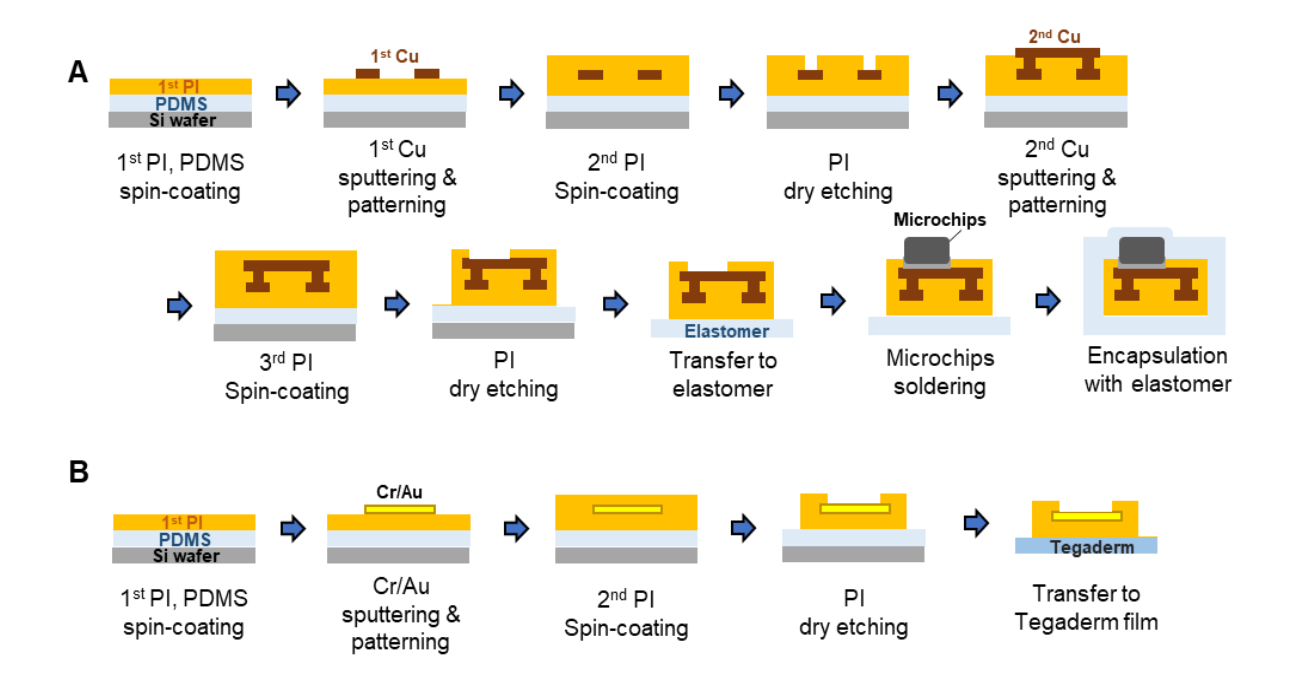


**Fig. S2.** Illustration of microfabrication processes of SKINTRONICS. A) Stretchable serpentine-patterned circuit and B) open-mesh nanomembrane electrodes.

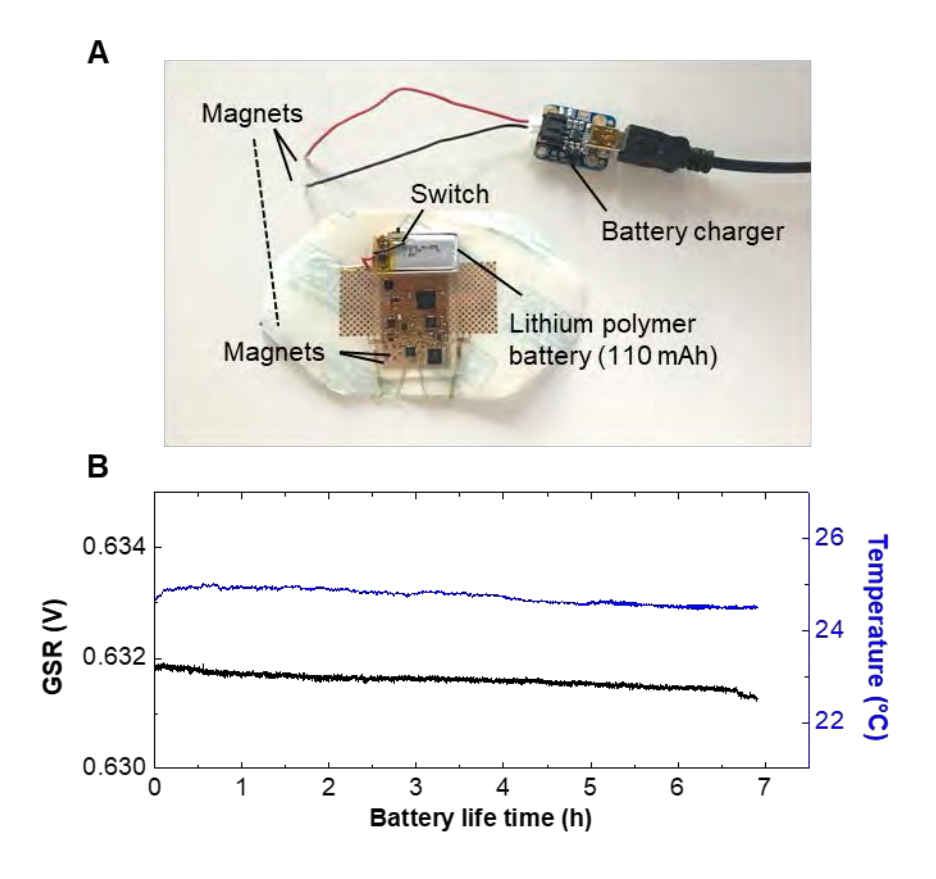


**Fig. S3.** A) SKINTRONICS with a rechargeable lithium-polymer battery and charging unit. The circuit and battery charger can be connected through small magnets. B) Device operation time with the miniature battery; both GSR and temperature signals can be recorded for 7 hours.

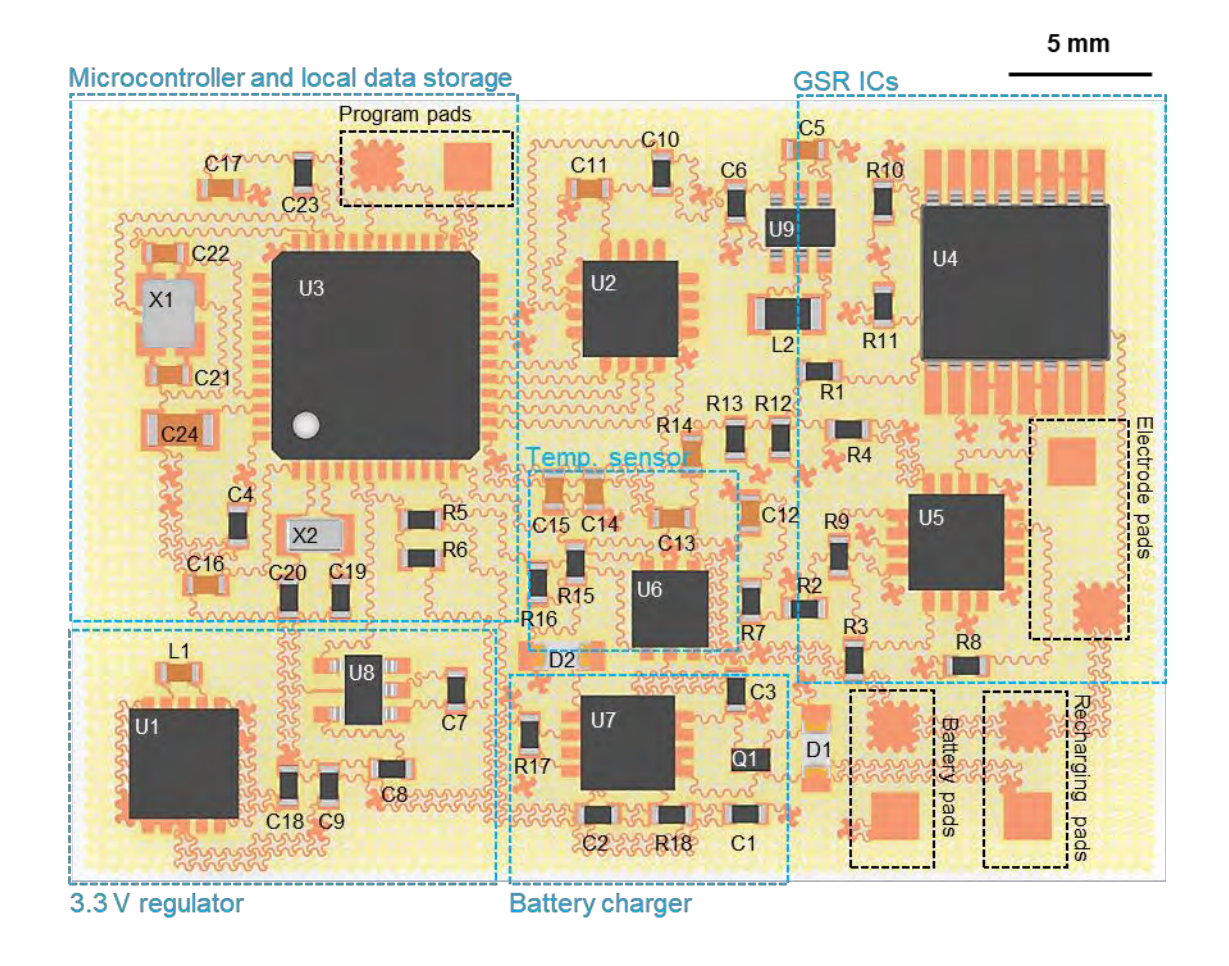


**Fig. S4.** Top-view illustration of the SKINTRONICS circuit with multiple chip components. Details of the circuit components appear in Table S1.

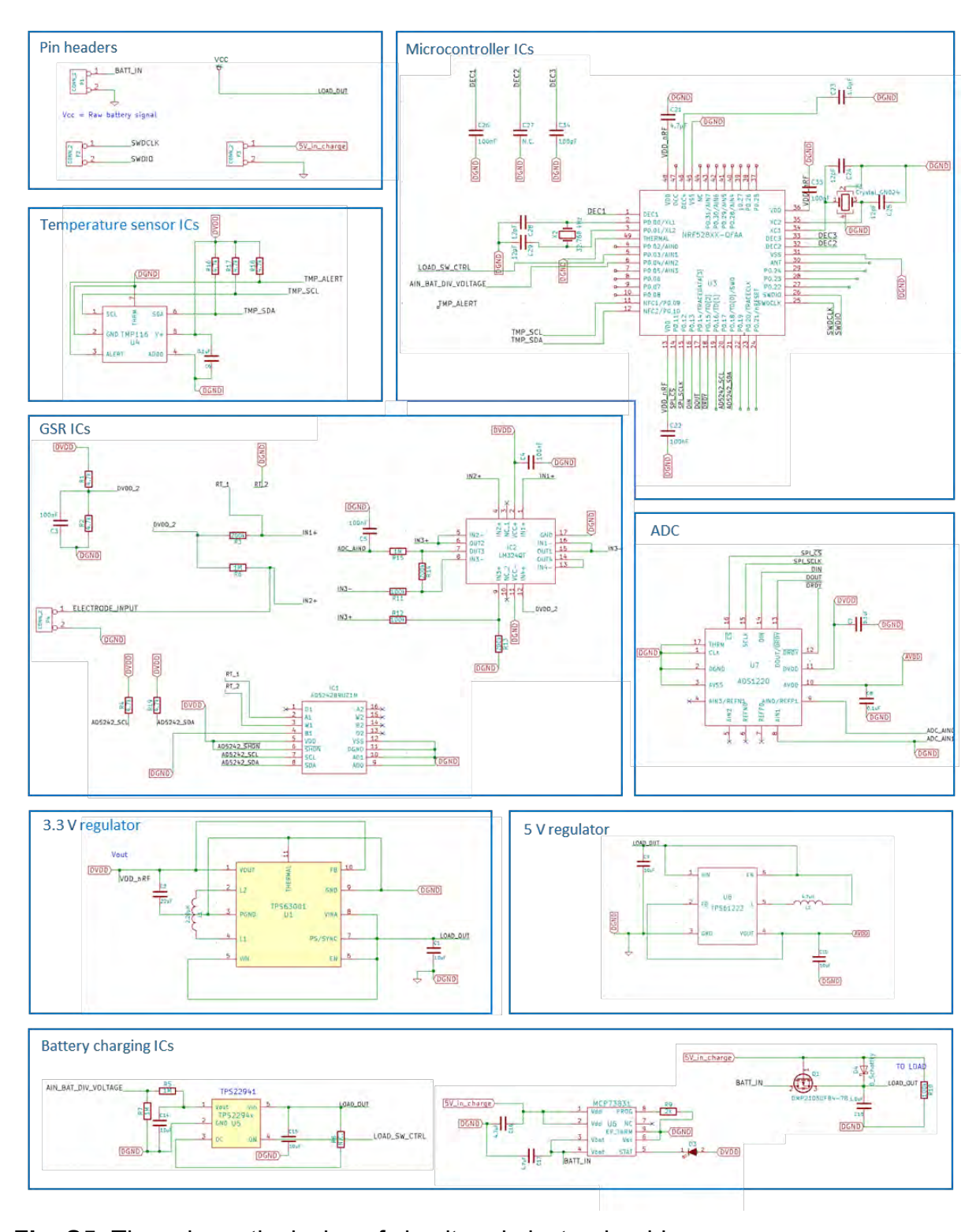
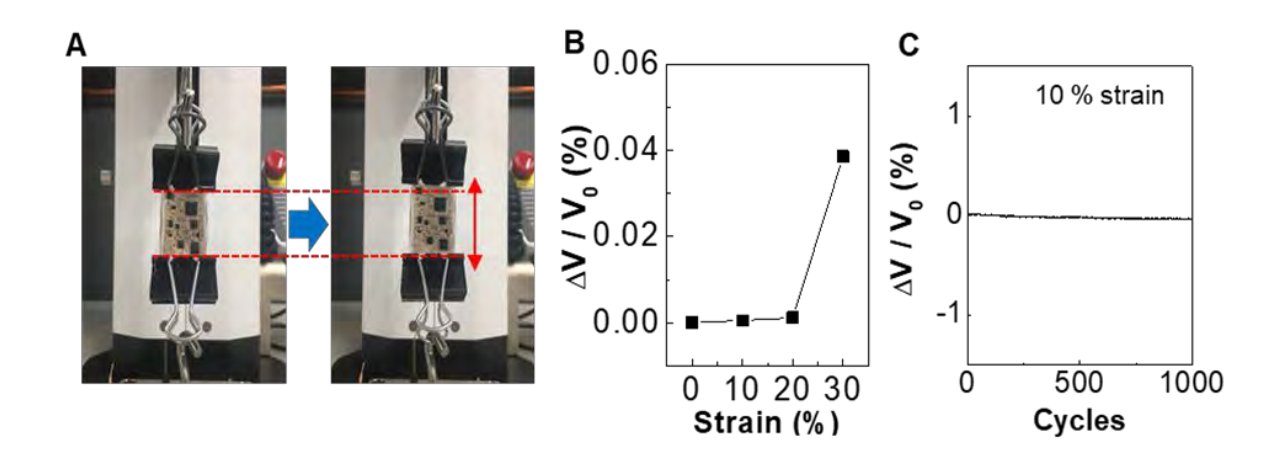
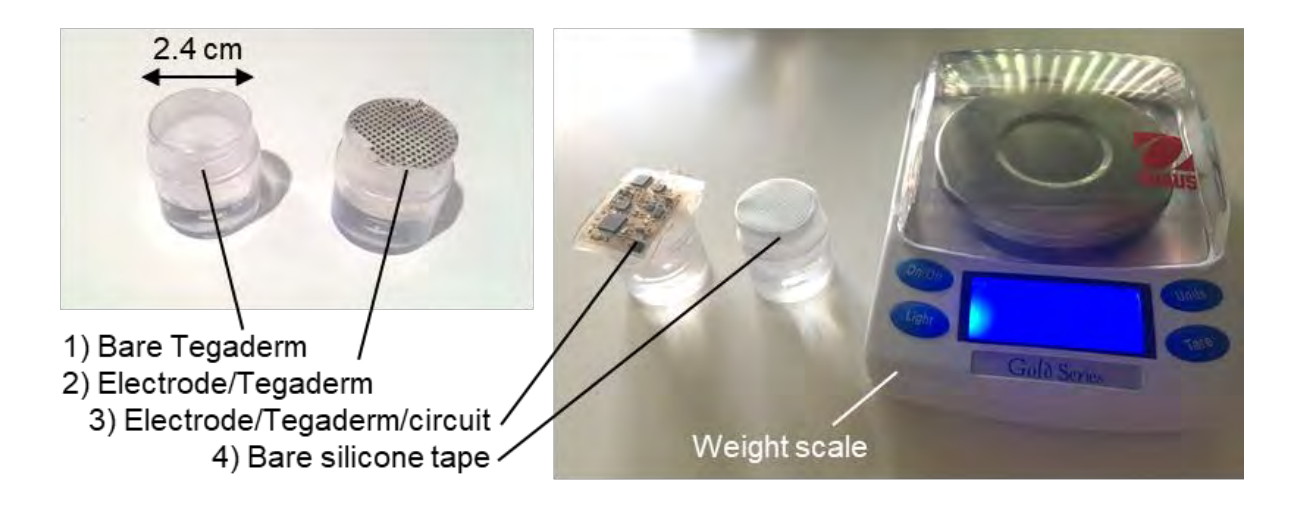


Fig. S5. The schematic design of circuit and electronic wiring.



**Fig. S6.** A) Cyclic loading mechanical tester. B) Voltage change of the device upon tensile loading, showing negligible differences up to 20% elongation. C) Cyclic loading for 1,000 cycles with a 10% strain assures the device's mechanical reliability.



**Fig. S7.** Experimental setup for breathability with four types of membranes. Plastic bottles with water are covered by each membrane and tightened by a film. For membrane type 3), the fabricated circuit that can fully cover the bottle's inlet is also attached to type 2) structure. The bottles are placed in a controlled environment with consistent temperature and humidity, 24°C and 50%, respectively. The weight scale measures the water loss of each case.

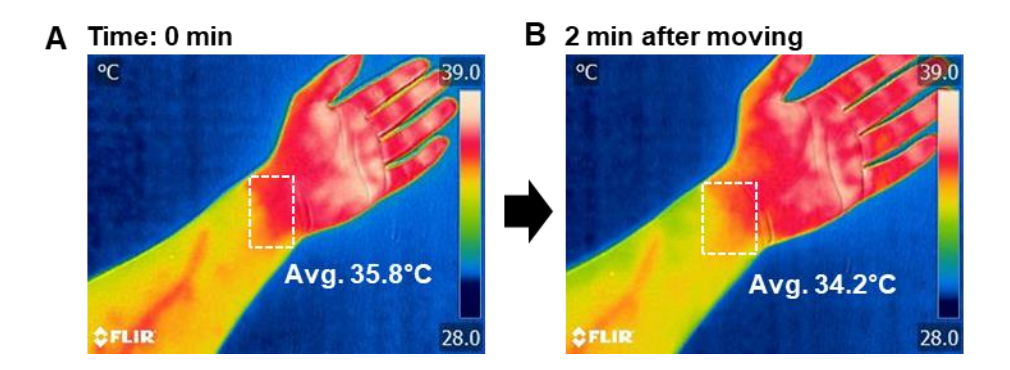


**Fig. S8.** Temperature variation regarding moving activity measured by infrared camera (E8, FLIR). A) Thermal images on the wrist before and B) after 2 minutes of moving in an indoor environment, which shows temperature reduction.

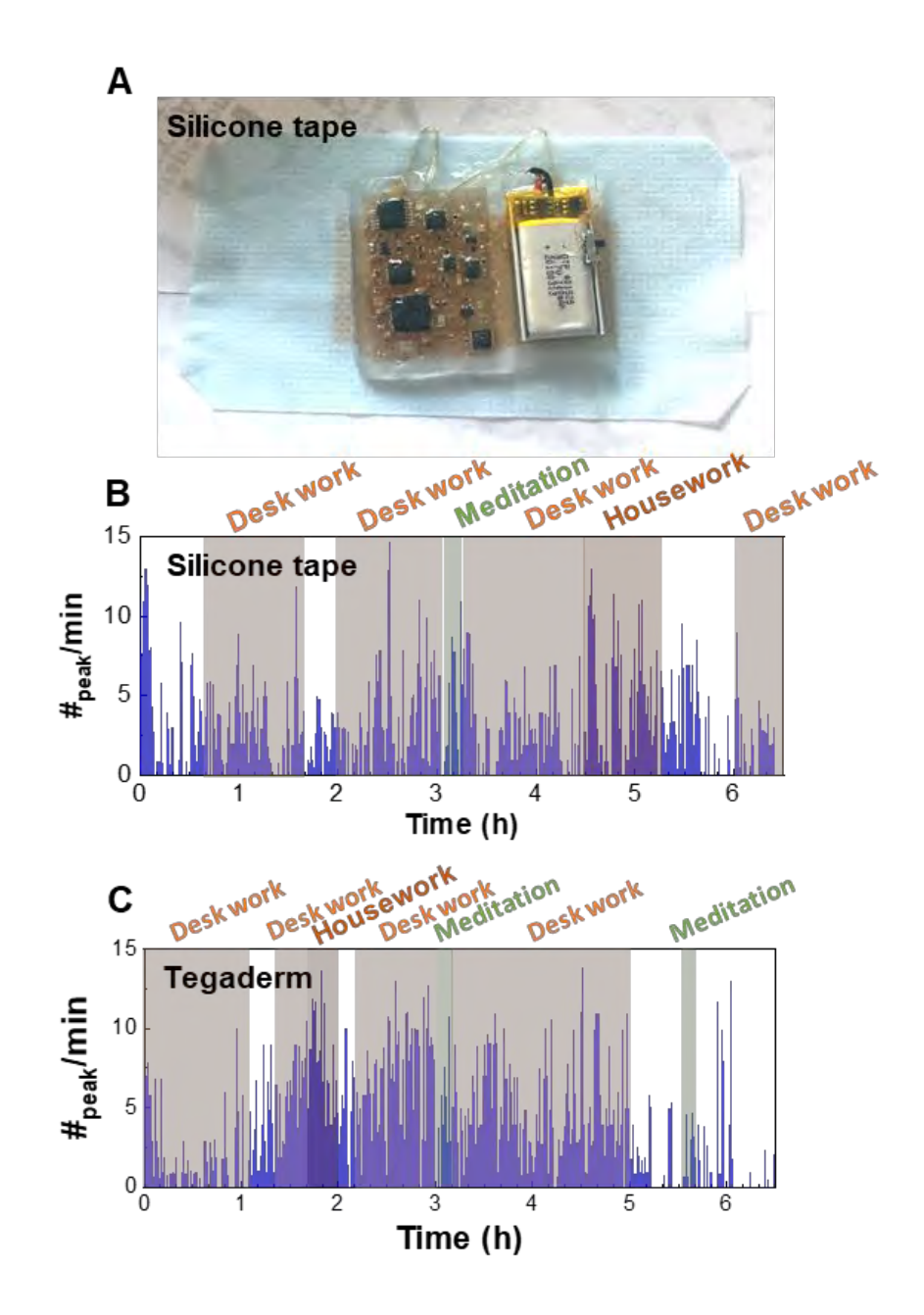


**Fig. S9.** A) SKINTRONICS integrated by a reusable silicone tape (Kind Removal, 3M). B-C) GSR data measured over 6 hours during multiple daily activities with a device on B) a reusable silicone tape and C) a signle-use thin film (Tegaderm).

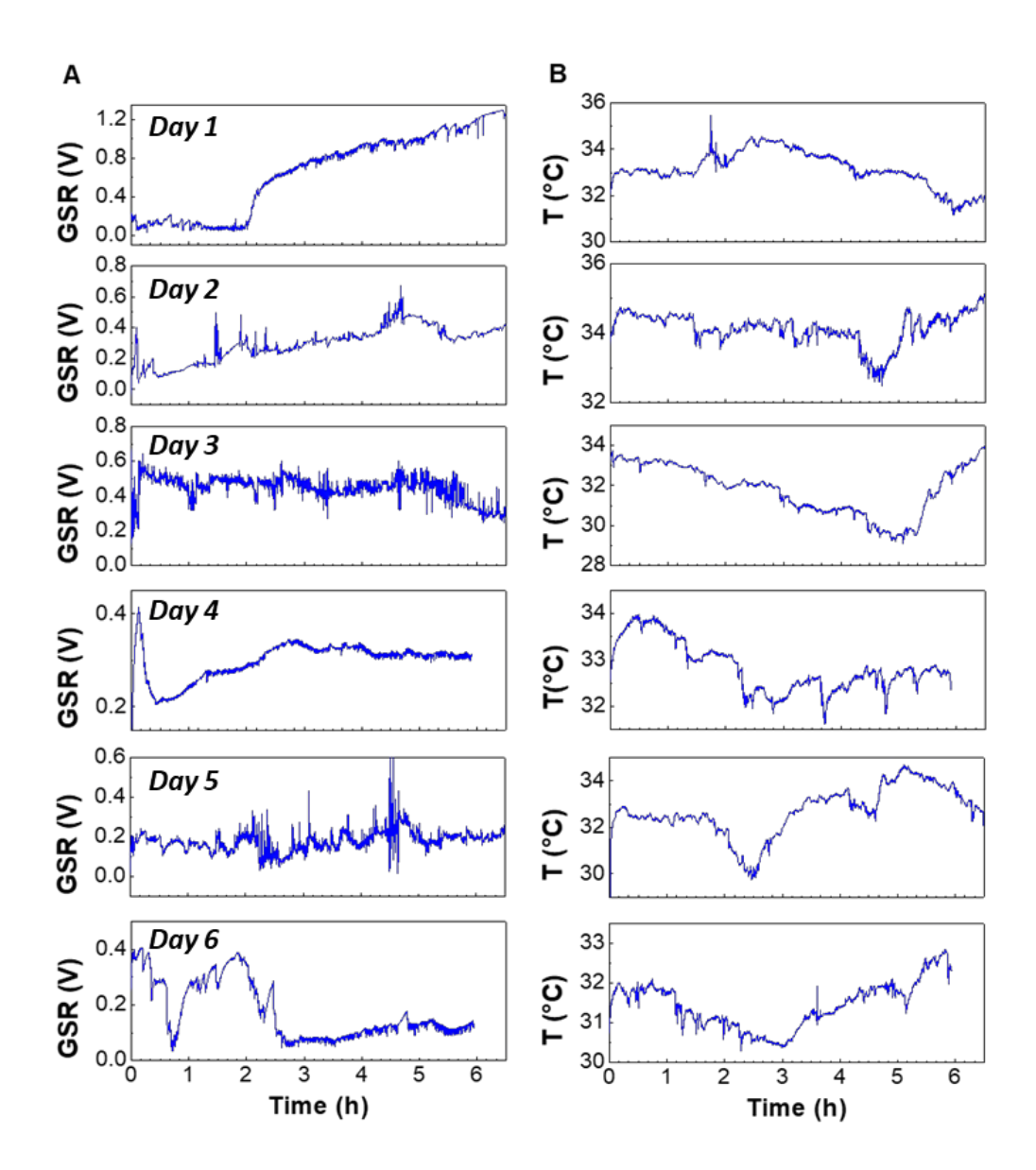


**Fig. S10.** Measured GSR and temperature data from subject #1. A) Raw GSR signals and B) Skin temperature signals for 6 hours per day for six consecutive days.

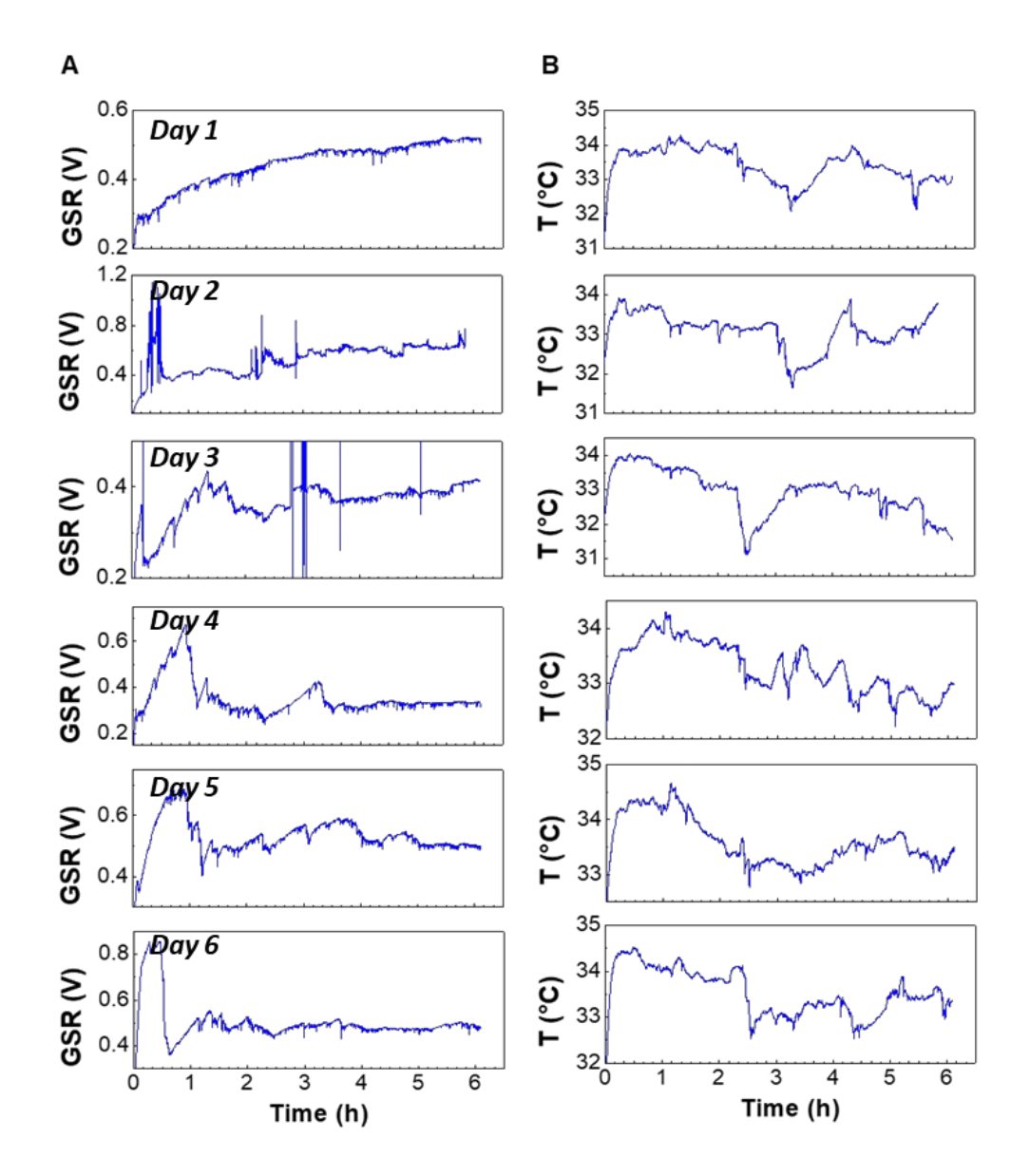


**Fig. S11.** Measured GSR and temperature data from subject #2. A) Raw GSR signals and B) skin temperature signals for 6 hours per day for six consecutive days.

 Table S1. List of chip components used for the SKINTRONICS circuit.

Component	Description	Value	Part number
U1	3.3 voltage regulator	N/A	TPS63001
U2	Analog front-end	N/A	ADS 1220
U3	Microcontroller	N/A	Nrf52832-QFAA-R
U4	Digital potentiometer	N/A	AD5242
U5	Op-amp	N/A	LM324QT
U6	Temperature sensor	N/A	TMP116
U7	Charging controller	N/A	MCP73831
U8	Current limit active-low load switch	N/A	TPS22941
U9	5 V regulator	N/A	TPS61222
X1	32 MHz crystal	N/A	ECS-320-8-37CKM
X2	32.768 kHz crystal	N/A	ECS-327-9-12-TR
Q1	MOSFET	N/A	DMP21D5UFB4-7B
D1	Schottky diode	N/A	CDBU0530
D2	LED	N/A	LTST-C1O94TBKT
R1 - R3	0402 resistor	200 kΩ	N/A
R4 - R7	0402 resistor	1 ΜΩ	N/A
R8, R9	0402 resistor	100 kΩ	N/A
R10 - R16	0402 resistor	4.7 kΩ	N/A
R17	0402 resistor	2 kΩ	N/A
R18	0402 resistor	13 kΩ	N/A
C1	0402 capacitor	1.0 uF	N/A
C2 - C4	0402 capacitor	4.7 uF	N/A
C5 - C9	0402 capacitor	10 uF	N/A
C10 - C17	0402 capacitor	0.1 uF	N/A
C18	0402 capacitor	22 uF	N/A
C19 - C22	0402 capacitor	12 pF	N/A
C23	0402 capacitor	0.1 nF	N/A
C24	0603 capacitor	1 uF	N/A
L1	0402 inductor	2.2 nH	N/A
L2	0603 inductor	4.7 uH	N/A

**Video S1.** Real-time, continuous monitoring of GSR and temperature during meditation and desk work.

